Universality classes for deterministic surface growth

J. Krug* and H. Spohn*

Institute for Theoretical Physics, University of California, Santa Barbara, California 93106

(Received 29 February 1988)

We study the growth of a surface through deterministic local rules. A scaling theory for the generalized deterministic Kardar-Parisi-Zhang equation $\partial_t h = D \Delta h + \lambda |\nabla h|^\beta$, with $\beta \geq 1$, is developed. A one-dimensional surface model, which corresponds to $\beta = 1$, is solved exactly. It can be obtained as a limiting case of ballistic deposition, or as the deterministic limit of the Eden model. We determine the scaling exponents, the correlation functions, and the skewness of the surface. We point out analogies to the Burgers equation ($\beta = 2$), for which such detailed properties are not known.

I. INTRODUCTION

An important growth mechanism for surfaces is through ballistic deposition. The somewhat simple-minded, theoretical picture is that particles in the ambient atmosphere move ballistically towards the surface. As a particle reaches the surface it has a certain probability to stick at the surface. This sticking probability depends on the local surface configuration. From the point of view of the surface, it grows through a stochastic mechanism governed by (approximately) *local* rules. It is the locality of the growth mechanism which makes ballistic deposition distinct from diffusion-limited aggregation.

In all the local growth rules considered so far, the deposit is never fractal, although its density may be smaller than the density of the substrate. Therefore the interest focuses on the structure of the surface itself. One expects the surface to be statistically self-similar on a large space-time scale, i.e., over distances large compared to typical sizes of the deposited particles and over times long compared to typical aggregation times. Just as in equilibrium critical phenomena, self-similarity is characterized by scaling exponents and functions. We would like to understand how the large scale properties of the surface depend on the local growth rules. Numerical simulations establish that (i) the scaling properties of the growing surface differ from a surface in thermal equilibrium[1-5] and (ii) the scaling properties depend on the local rule.[6,7]

As a first orientation, let us consider the random deposition model.[1,6] Above each site of a reference lattice we give a surface height $h_i(t)$ as a function of time. Each $h_i(t)$ grows independently according to a Poisson process. The average height (=average mean deposit per lattice site) grows linearly in t. Starting with a flat surface, its width increases indefinitely as $\sqrt{t}$. The surface is spatially uncorrelated.

Clearly, the simplicity of the model is due to the absence of any interaction between different lattice sites. Edwards and Wilkinson[8] derived a *linear* Langevin equation for surface deposition which takes into account some local rearrangement of the deposited particles. As a re-

sult, correlations build up in the surface. The surface width w then evolves according to the scaling form[1]

$$w(L,t) = L^\zeta f(t/L^z) , \qquad (1.1)$$

where L is the size of the substrate, ζ and z are scaling exponents (cf. Sec. II), and the scaling function $f(x)$ has the asymptotics $f(x \to \infty) = \text{const}$, $f(x \to 0) \sim x^{\zeta/z}$. However, the exponents obtained from the linear theory do not agree with numerical simulations. Kardar, Parisi, and Zhang[9] (KPZ) argued that a nonlinear term must be included to account for lateral growth. They proposed the following equation for the dynamics of the surface:

$$\frac{\partial}{\partial t} h(x,t) = c + D \Delta h(x,t) + \lambda [\nabla h(x,t)]^2 + \eta(x,t) \qquad (1.2)$$

(KPZ equation). $h(x,t)$ is the height of the surface at time t above the point x in the reference plane. c is the growth speed and $\eta(x,t)$ is white noise in space time,

$$\langle \eta(x,t)\eta(x',t') \rangle = \sigma^2 \delta(x-x')\delta(t-t') . \qquad (1.3)$$

Going to a frame of reference moving with velocity c, we may set $c = 0$ in (1.2). $D \Delta h$ describes diffusional relaxation within the surface. D is the diffusion coefficient. The strength of the nonlinearity λ is proportional to the growth speed. The surface gradient ∇h is governed by the well-known Burgers equation[10] with noise.

With $\lambda = 0$, (1.2) reduces to the equation of Edwards and Wilkinson, whereas $\lambda = 0$, $D = 0$ corresponds to the random deposition model. Simulations of various local growth rules in two dimensions (=one-dimensional surface) suggest that (1.2) with $\lambda \neq 0$ correctly describes the large-scale properties of these models.[2-4] However, we are far from understanding which set of growth rules lead to the KPZ equation in the continuum limit. Even worse, the scaling properties of the KPZ equation itself are well known only in two dimensions.[9,11,12] For higher dimensions there is only a scaling relation[11,13] reducing the problem to a single scaling exponent. In three dimensions the numerical data for the exponents scatter by about 15%.[2,5,13]

In the present paper we investigate the KPZ equation and related models without noise. *With* noise, the KPZ equation describes (statistically) steady growth in the long time limit. However, *without* noise, the KPZ equation models the relaxation of an initially rough surface to a flat surface. If the initial data are statistically scale invariant, this relaxation proceeds in a self-similar fashion. The large-scale properties of the surface are then governed by scaling exponents very much like in the stochastic case. In order to account for different universality classes, we develop a scaling theory for the deterministic KPZ equation with general nonlinearity $|\nabla h|^\beta, \beta \geq 1$ (Sec. II). The results of Burgers[10] are obtained as a special case. In Sec. III we introduce a particular local growth rule. In fact, it is essentially identical to the elementary cellular automaton 184 in Wolfram's classification.[14] We show that this model belongs to a *different* universality class than the standard KPZ equation (1.2) and verify the predictions of the scaling theory. The surface correlations are obtained exactly, and the surface is shown to be asymmetric with respect to the direction of growth. Finite-size effects are also evaluated. In Sec. IV we investigate the deterministic limit of the Eden model. Some conclusions are given in Sec. V.

II. SCALING THEORY FOR DETERMINISTIC SURFACE GROWTH

Let us first consider quite generally the scaling properties of a surface evolving through some stochastic or deterministic process. We fix a typical length scale $\xi_\parallel$ parallel to the substrate. $\xi_\parallel$ could be the side length of the system or the correlation length parallel to the substrate. There are then two natural questions to be asked.

(i) What is the typical magnitude $\xi_\perp$ of surface fluctuations perpendicular to the substrate which one observes over the distance $\xi_\parallel$? For a (statistically) scale invariant surface $\xi_\perp$ and $\xi_\parallel$ have to be related by

$$\xi_\perp \sim \xi_\parallel^\zeta , \tag{2.1}$$

where ζ, $0 \leq \zeta < 1$, is the wandering or roughness exponent.[15] Clearly, ζ describes the *static* scaling properties of the surface.

(ii) What is the typical time τ which is required for a surface fluctuation to spread over the distance $\xi_\parallel$? Dynamic scaling implies then

$$\tau \sim \xi_\parallel^z , \tag{2.2}$$

where z is the *dynamic* exponent.

Within this general framework we would like to understand the scaling properties of deterministic surface growth subject to random initial data. Since we expect the scaling exponents to depend crucially on the form of the nonlinearity, we generalize the deterministic KPZ equation to

$$\frac{\partial h}{\partial t} = D\nabla^2 h + \lambda |\nabla h|^\beta , \tag{2.3}$$

$\beta \geq 1$. $\beta = 2$ is the standard KPZ equation discussed in the Introduction. The initial conditions are chosen from

an ensemble of random surfaces characterized by the covariance

$$\langle |h(x) - h(x')| \rangle \sim |x - x'|^{\bar\zeta} \tag{2.4}$$

for $|x - x'|$ large with some scaling exponent $\bar\zeta$, $0 \leq \bar\zeta < 1$.

Since the deterministic dynamics is purely relaxational and does not generate any proper steady state, we expect the static scaling exponent ζ introduced in the preceding paragraph to be determined by the scale invariance of the initial data, i.e., $\zeta = \bar\zeta$. This is most easily illustrated for the diffusive relaxation $\lambda = 0$ in (2.3). Then the amplitude of a surface mode with wave vector q, $\hat h(q,t)$, decays according to

$$|\hat h(q,t)|^2 = |\hat h(q,0)|^2 e^{-2Dq^2 t} . \tag{2.5}$$

Thus the solution factorizes into a static part completely determined by the initial condition, and a dynamic part which displays dynamic scaling with $z = 2$ irrespective of the initial data. In the following we shall therefore treat the static exponent ζ as an input parameter given by the choice of initial conditions.

The relaxation process described by (2.3) is associated with a growth of correlations in the system. The corresponding correlation length $\xi(t)$ is the distance over which smoothing has been effective up to time t. It can be identified with the parallel length scale $\xi_\parallel$ introduced above. Accordingly it grows in time as

$$\xi \sim t^{1/z} . \tag{2.6}$$

To characterize the relaxational process we consider the decay of the density of surface steps, defined by

$$\rho(t) := \frac{1}{L^{d-1}} \int d^{d-1}x \langle |\nabla h(x,t)| \rangle . \tag{2.7}$$

Here L denotes the linear size of the substrate, and the brackets denote averaging with respect to the ensemble of initial conditions. Since a typical slope of the surface is proportional to $\xi_\perp/\xi_\parallel$, we conclude from the general scaling picture that

$$\rho(t) \sim \xi_\parallel^{\zeta-1} \sim t^{-(1-\zeta)/z} . \tag{2.8}$$

Another quantity of interest is the mass deposited per unit area up to time t,

$$m(t) = \frac{1}{L^{d-1}} \int d^{d-1}x \langle h(x,t) - h(x,0) \rangle . \tag{2.9}$$

[Note that in (2.3) the uniform part of the mass density, growing as ct, has been subtracted.] Since the Laplacian in (2.3) does not contribute to (2.9), we see from (2.3) that $(d/dt)m(t) \sim \rho(t)^\beta$, i.e., using (2.8),

$$m(t) \sim t^{1-[\beta(1-\zeta)]/z} . \tag{2.10}$$

For any finite sample the growth eventually terminates, as the surface has become completely flat. According to our general scaling hypothesis, the corresponding relaxation time T should be proportional to L^z. Thus the growth law (2.10) saturates at some value $m_{\max}$, which is given by

$$m_{\max} \sim T^{1-[\beta(1-\zeta)]/z} \sim L^{z-\beta(1-\zeta)} \ . \tag{2.11}$$

There is another way to estimate $m_{\max}$. To this end we note that the process described by (2.3) is essentially a filling process, in the sense that local minima are elevated, whereas flat portions of the surface do not propagate. Thus we expect $m_{\max}$ to be of the same order as the maximum height difference in the initial surface configuration. With (2.4) this implies

$$m_{\max} \sim L^\zeta \ . \tag{2.12}$$

Comparing (2.11) and (2.12) we then obtain an expression for z in terms of β and ζ,

$$z = \zeta(1-\beta)+\beta \ . \tag{2.13}$$

We note that the scaling relation (2.13) is independent of dimension. Also for $\beta=1$, z does not depend on ζ. If $\zeta(1-\beta)+\beta>2$, then the z of (2.13) becomes *larger* than the diffusive value $z=2$. As a consequence, the diffusive surface relaxation due to the Laplacian in (2.3) occurs *faster* than the nonequilibrium process described by the nonlinearity, thus dominating the asymptotic decay of the step density $\rho(t)$. We conclude therefore that a nonlinear term with $\beta \geq (2-\zeta)/(1-\zeta)$ is irrelevant to the long-time behavior of (2.3) subject to initial data with roughness exponent ζ. For the deterministic KPZ equation $\beta=2$, the scaling relation becomes

$$z = 2-\zeta \ . \tag{2.14}$$

This has been derived previously for the stochastic KPZ equation.[11,13] It thus appears to be a general feature of the gradient-squared nonlinearity.

In the following sections we will restrict ourselves to two-dimensional models and to initial data with $\zeta=\frac{1}{2}$. It has been shown both for the stochastic KPZ equation[9] and for various lattice growth models[2,3] that the static scaling exponent equals $\zeta=\frac{1}{2}$ in two dimensions. This implies that the surface increments at different positions are uncorrelated. Equivalently, these surface configurations may be viewed as graphs of one-dimensional random walks. With $\zeta=\frac{1}{2}$ (2.13) reduces to

$$z = (1+\beta)/2 \ . \tag{2.15}$$

For $\beta \geq 3$ the nonlinearity is irrelevant. For $\beta=2$ we recover the familiar anomalous exponent $z=\frac{3}{2}$ of the Burgers equation,[10] (cf. also Sec. V. The case $\beta=1$ will be studied in detail in Sec. III).

III. AN EXACTLY SOLVABLE LATTICE MODEL

We introduce and study a cellular automaton which can be understood as a discrete version of the KPZ equation with nonlinearity $|\nabla h|$. The spatial dimension is $d=2$, and the surface is a line. Whereas a general nonlinearity $|\nabla h|^\beta$ seems to be difficult to handle analytically, the particular case $\beta=1$ can be studied in great detail. In fact, we will not only verify the scaling picture, but also determine the locally asymmetric structure of the surface and finite-size effects.

A. Definition of the lattice model

The cellular automaton to be studied may be thought of as a limiting case of standard ballistic deposition. Consider a one-dimensional surface configuration parallel to the x axis of a square lattice [Fig. 1(a)]. Particles move on straight lines along the y axis and become part of the deposit when they reach the empty nearest neighbor of an occupied site. Thus an incoming particle may stick either to the side edge or to the top edge of an existing column. Now an incoming particle may not stick at all to the surface, but rather reenter the ambient atmosphere. Therefore it is realistic to attribute different rates, Γ_{side} and Γ_{top}, to the two sticking processes. We also introduce the ratio $p = \Gamma_{top}/\Gamma_{side}$. In the limit $p \to \infty$ one recovers the
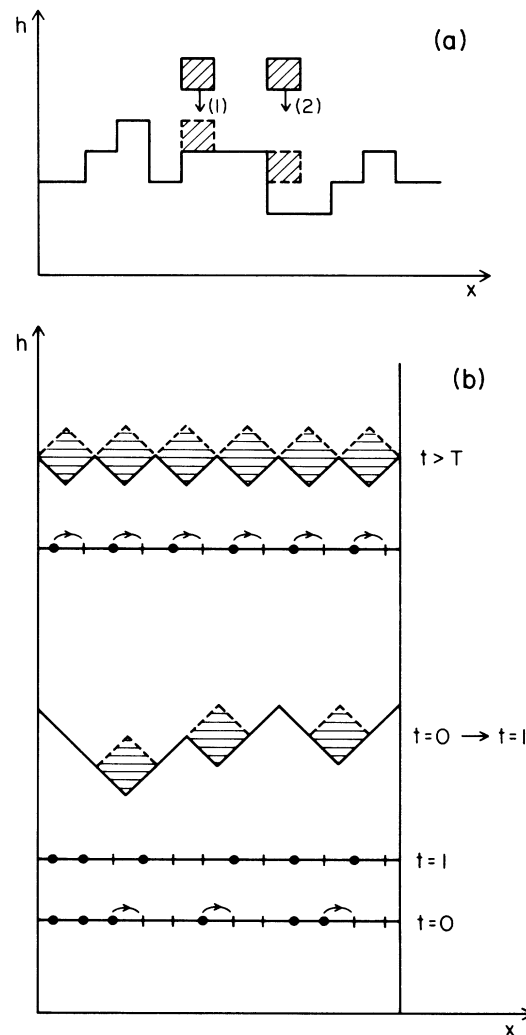
FIG. 1. (a) On-lattice ballistic deposition with varying sticking probabilities. Process (1) occurs at rate Γ_{top}; process (2) at rate Γ_{side}. (b) Deterministic growth from a rough surface parallel to the (1,1) direction. At each time step, all local surface minima are filled with new particles. The corresponding lattice gas evolves according to the automaton rule 184. For $t > T$, the surface is flat and the automaton is in the ordered antiferromagnetic state.

random deposition model, where the columns grow independently according to a Poisson process.[1,6] Here we consider the opposite limit $p \to 0$. Then, as particles are allowed to stick only to the corners of existing surface steps, a flat surface clearly cannot grow. A rough surface with a finite density of steps will be smoothed by the process until, for any finite sample, no steps are left and the growth terminates. It is this nonequilibrium annealing process that we will study.

Having specified the local growth rule, we must now give the updating procedure. As we want to study the deterministic evolution of a random initial configuration, we suppress any temporal noise by *simultaneously* updating all lattice sites from one time step to the next. We do not expect our results to depend on this choice, since the present growth rule leads to a decay of the density of steps irrespective of the updating procedure. To see this, just note that it is impossible to create new steps, whereas pairs of steps annihilate each other at local minima of the surface. Indeed, we have checked numerically that random sequential updating merely renormalizes the time scale of the process, without affecting the detailed dynamic scaling properties.[16] This behavior is very different from some other growth models, where the random choice of the actual growth site at each time step is the source of large-scale fluctuations of the interface, cf. Sec. III B.

With simultaneous updating, the interface dynamics can be written in the following simple form:

$$h_i(t+1) = \max(h_{i-1}(t), h_i(t), h_{i+1}(t)) , i = 1, \ldots, L$$

$$(3.1)$$

where $h_{L+1}(t) = h_1(t)$. $h_i(t)$ denotes the height of the surface at the lattice site i at the (integer) time t. It is useful to introduce the surface step variables

$$\sigma_i(t) = h_{i+1}(t) - h_i(t) .$$

$$(3.2)$$

The way we motivated the model, $h_i(t)$ [and $\sigma_i(t)$] have to be integer valued, and it is this case which will be studied in the sequel. In fact we will adopt the further simplification $\sigma_i(t) = 0, \pm 1$. However, the large-scale properties of surfaces governed by Eq. (3.1) are independent of such details provided only the initial surface looks like the graph of a random walk.

Let us then specify the precise ensemble of initial surface configurations. At each lattice site i we choose $\sigma_i(0)$ independently to be ± 1 with equal probability. In order to have a surface configuration which satisfies periodic boundary conditions, we impose the additional constraint

$$\sum_{i=1}^{L} \sigma_i(0) = 0 .$$

$$(3.3)$$

(L has to be even.) The resulting surface is then simply the graph of a one-dimensional symmetric random walk which moves along the h axis in time i and returns to the initial position at time $i = L$. In particular, the mean-square fluctuation of the surface around the average height is easily shown to be

$$w(L)^2 = \frac{L}{12} .$$

$$(3.4)$$

Thus the ensemble is characterized by the static exponent

$$\zeta = \frac{1}{2} .$$

$$(3.5)$$

We also want to determine the dynamic exponent z. One method would be to expand the right-hand side of (3.1) in gradients in order to find out the value of β. A more direct approach is to note that, without further approximation, the step density

$$\rho(t) = \frac{1}{L} \sum_{i=1}^{L} |\sigma_i(t)|$$

$$(3.6)$$

is related to the total mass $m(t)$ deposited up to time t by

$$m(t) = \int_0^t ds \, \rho(s) ,$$

$$(3.7)$$

since each surface step accommodates exactly one new particle. Therefore we conclude

$$\beta = 1$$

$$(3.8)$$

and according to our scaling theory

$$z = 1 .$$

$$(3.9)$$

To actually compute correlation and scaling functions, the clue is to consider the dynamics of surface steps. We note that since $|\sigma_i(0)| = 1$, $\sigma_i(t) = 0, \pm 1$ for all t under the dynamical rule (3.1). Clearly, $\sigma_i = 1$ if there is an upward step at site i, $\sigma_i = -1$ if there is a downward step, and $\sigma_i = 0$ if no step is present. When a particle is deposited next to an upward step, the step moves to the left, whereas a downward step moves to the right. If a particle is deposited at a local minimum where two steps of different sign oppose each other, they are annihilated. Thus the upward and downward steps behave like a collection of "particles" with velocities ± 1, which annihilate each other. Initially the particles have an ideal gas distribution.

In this picture the density of steps $\rho(t)$ is then simply the total density of particles. Obviously, $\rho(t)$ decreases in time and must eventually vanish in any finite system.

B. The cellular automaton 184

Before turning to the computation of step correlation functions, we would like to point out a surprising connection of (3.1) to a seemingly very different deterministic dynamical system. Let us introduce a slightly modified version of our model. We consider deposition onto a one-dimensional surface parallel to the (1,1) direction of a square lattice [Fig. 1(b)]. The particles are allowed to stick only at the local minima of the surface. It is easy to see that the surface configurations generated have local gradients ± 1. By adding a particle at site i the gradients at the bonds $(i-1, i)$ and $(i, i+1)$ are interchanged. Thus the model is equivalent to a kinetic Ising model with asymmetric spin-exchange dynamics.[17] Because of the conservation law the particle language is more convenient. We set the local surface gradients equal to $2\eta_i - 1$, $\eta_i = 0, 1$. $\eta_i = 1$ (0) means that lattice site i is oc-

cupied (empty). The particles have a simple dynamics. With rate 1 they jump to the right except when the final site is occupied, in which case they stay (hard-core exclusion). This is also called the single-step model. It has been studied both numerically and analytically.[2,3,12] Here we consider the *deterministic* version. In a single time step every particle moves to the right subject to the hard-core exclusion. The configuration $\eta_i(t+1)$ at time $t+1$ is determined from the configuration $\eta_i(t)$ by a local rule which depends on nearest neighbors only. This is precisely the definition of an elementary cellular automaton as introduced by Wolfram.[14] In his notation the deterministic driven lattice gas evolves according to the rule 184. For long times the dynamics leads to a trivial limit cycle. For that reason the automaton 184 has been dismissed as "not interesting." However, as we will see, the approach to the final state has a rich spatiotemporal structure, especially when interpreted as a surface.

It remains to establish the connection to the lattice model of Sec. III A. For the half-filled lattice in the steady state of the automaton, every other site is occupied. This corresponds to a "flat" interface along the (1,1) direction, equivalent to the ordered antiferromagnetic state of the lattice gas. To describe the relaxation into the steady state, we introduce variables which vanish in the ordered regions. Hence

$$\sigma_i(t) := \eta_i(t) + \eta_{i+1}(t) - 1 \ . \tag{3.10}$$

Then $\sigma_i(t) = 0, \pm 1$, and $|\sigma_i(t)| = 1$ only if either two particles or two vacancies occupy adjacent sites. It is straightforward to check that the dynamics of the $\sigma_i(t)$ is identical to that of the step variables (3.2) governed by Eq. (3.1).

In the lattice gas variables, the particles with velocity ± 1 may be thought of as kinks and antikinks which separate ordered regions where $\sigma_i(t) = 0$. Thus the ordering of the lattice gas proceeds through the decay of the kink density $\rho(t)$ defined by (3.6). A similar problem was studied by Grassberger for the elementary automaton 18.[18] However, due to the strong correlations between kinks, the decay of $\rho(t)$ is not simply related to the growth of some typical domain size $l \approx 1/\rho$ as one might have expected.

It should be mentioned that our deposition model is in essence equivalent to a two-species annihilation reaction, $A + B \rightarrow$ inert, where A and B particles move with a relative drift, in one dimension. Reactions of this type have been studied by Kang and Redner.[19] No attempt to investigate correlations has been made, however.

Let us comment on the random sequential updating of the automaton 184. In this case the lattice gas reaches in the course of time a steady state, where each lattice site is independently occupied with probability $\frac{1}{2}$. The surface grows then steadily and is characterized by the roughness exponent $\zeta = \frac{1}{2}$. In the continuum approximation, the model is described by the standard KPZ equation (1.2) with a gradient-squared nonlinearity.[3,17] Accordingly, the dynamic exponent is $z = \frac{3}{2}$, but it no longer describes the relaxation to a flat surface. Thus we see that random updating not only is a relevant source of noise in this

model, but it also changes the power of the nonlinearity and thereby the universality class.

C. Step correlations and surface structure in the infinite system

The principle of how to obtain correlation functions is most clearly illustrated by computing the asymptotic decay of the step density $\rho(t)$, cf. (3.6). We study directly the infinite system $L \rightarrow \infty$. The distribution of the $\sigma_i(0)$'s is translation invariant, a property which is preserved in the course of time. Therefore $\rho(t)$ is the probability to find a particle at the origin (or any other lattice site) at time t. Let us assume that the particle at the origin has velocity $+1$ (-1 follows by symmetry). This particle must have started at time $t = 0$ at the position $i = -t$. It also has to be annihilated only after time t. This condition constrains the particles initially present in the interval $[-t, t]$ by

$$\sum_{i=-t}^{x} \sigma_i(0) = h_x(0) - h_{-t}(0) < 0 \tag{3.11}$$

for all x with $-t \le x \le t$. Equation (3.11) ensures that the particle at the origin at time t will be annihilated by a particle which started outside $[-t, t]$ initially. Thus $\rho(t)$ equals the probability for a symmetric random walk not to return to the origin in $2t$ steps. This is a standard problem of random-walk theory, with the solution

$$\rho(t) = \frac{1}{\sqrt{\pi t}} \tag{3.12}$$

for large t. This confirms the scaling prediction (2.8) with $\zeta = \frac{1}{2}$ and $z = 1$.

The same method can be used to calculate the two-point step correlation function

$$G(l, t) = \langle \sigma_0(t) \sigma_l(t) \rangle \ , \tag{3.13}$$

$l \ge 0$. The constraint (3.11) is then replaced by a more involved restriction on the initial surface configuration $h_i(0)$. Leaving the computations to Appendix A, we quote only the final result, valid for large l and t,

$$G(l, t) = \frac{1}{\pi} \frac{1}{\sqrt{2tl}} f(l/\xi) \ , \tag{3.14}$$

with the correlation length

$$\xi := 2t \tag{3.15}$$

and

$$f(\lambda) = \begin{cases} \dfrac{1}{1+\lambda} & \text{for } \lambda \le 1 \\ 0 & \text{for } \lambda > 1 \ . \end{cases} \tag{3.16}$$

Equation (3.15) confirms that the dynamic exponent equals $z = 1$.

The functional form (3.14) is familiar from equilibrium critical phenomena. The correlations have a power-law decay up to some correlation length ξ, and decay much faster (usually exponentially) for $l > \xi$. Here the scaling function (3.16) drops discontinuously to zero at $l = \xi$. In fact, σ_0 and σ_l are statistically independent for $l > \xi$, i.e.,

$$\langle \sigma_0 \sigma_l \rangle = \langle \sigma_0 \rangle \langle \sigma_l \rangle = 0 \ , \tag{3.17}$$

cf. Appendix A. The critical limit $\xi \to \infty$ is, according to (3.15), identical to the long-time limit $t \to \infty$. This is a common feature of all growth models.[20]

An interesting consequence of (3.16) is that the step correlations are positive. This means qualitatively that given an upward (downward) surface step at site x, there is a strongly enhanced probability that the upward (downward) trend will continue over a range $x \pm 0(\xi)$. Instead of being composed of statistically-independent increments, we therefore expect the surface to consist of fairly straight segments extending over approximately ξ lattice spacings. As a direct measure of the height correlations we compute the mean-square fluctuations on the scale l,

$$\chi(l,t) := \langle [h_{x+l}(t) - h_x(t)]^2 \rangle$$
$$= \int_0^l dx \int_0^l dy \langle \sigma_x(t) \sigma_y(t) \rangle \ . \tag{3.18}$$

Inserting (3.14) into (3.18) we obtain for $l \leq \xi$

$$\chi(l,t) = \frac{8}{3\pi\sqrt{2t}} l^{3/2} F(l/\xi) \ , \tag{3.19}$$

with

$$F(\lambda) = \frac{3}{2\lambda} \left[\frac{1+\lambda}{\sqrt{\lambda}} \arctan(\sqrt{\lambda}) - 1 \right] \ , \tag{3.20}$$

whereas for $l > \xi$

$$\chi(l,t) = l - \left[\frac{4}{\pi} - 1 \right] \xi \ . \tag{3.21}$$

$\chi(l)$ is differentiable at $l = \xi$. The scaling function $F(\lambda)$ is nearly constant on the interval $[0,1]$, decreasing monotonously from $F(0) = 1$ to $F(1) = \frac{3}{2}(\pi/2 - 1) \simeq 0.856$. The result (3.19) confirms our expectations regarding the surface structure. The $l^{3/2}$ growth of χ is intermediate between the statistics of a random walk $(\chi \sim l)$ and that of a straight line segment $(\chi \sim l^2)$. Thus the surface is straightened on length scales $l \leq \xi$, with a sharp crossover to the random-walk behavior (3.21) at $l = \xi$.

At this point, it is useful to reconsider the notion of dynamic scale invariance introduced in Sec. II. According to the general scaling picture, we expect a surface characterized by scaling exponents ζ and z to be statistically self-similar with respect to the transformation

$$h'_x(t) = b^{-\zeta} h_{bx}(b^z t) \tag{3.22}$$

for any $b > 0$, i.e., h and h' should have the same statistics. In particular, all surface correlation functions should be invariant under (3.22). As we have argued above, $\zeta = \frac{1}{2}$ and $z = 1$ for our model. Thus $\chi(l,t)$ must satisfy the homogeneity relation

$$\chi(bl, bt) = b\chi(l,t) \tag{3.23}$$

which is indeed true both for (3.19) and (3.21).

To illustrate the dynamic scale invariance, we compare in Fig. 2 three surface configurations at times $t = 8$, 32, and 128, with the proper rescaling of the h and x axis in

accordance with (3.22). As expected, the qualitative appearance of the three surface profiles is the same. However, the pictures display some additional interesting features, the most notable being the asymmetry of the surface profiles under reflection, i.e., $h \to -h$. The reader is invited to turn the figures upside down to fully appreciate this effect. While such an asymmetry is generally to be expected in growth models with a preferred direction of growth—Eq. (2.3) is clearly not invariant under sign reversal of h—it has not been systematically studied in previous work. We will briefly comment on the possible occurrence of the effect in other, more realistic growth models at the end of this section.

A striking feature about the profiles in Fig. 2 are the plateaus at the local maxima of the surface, which almost all appear to be of the same width. A quantitative comparison reveals that this width equals the correlation length ξ. It is shown in Appendix A that the distance between an upward step and a downward step to the *right* of it, i.e., the width of a local maximum, is always *larger*
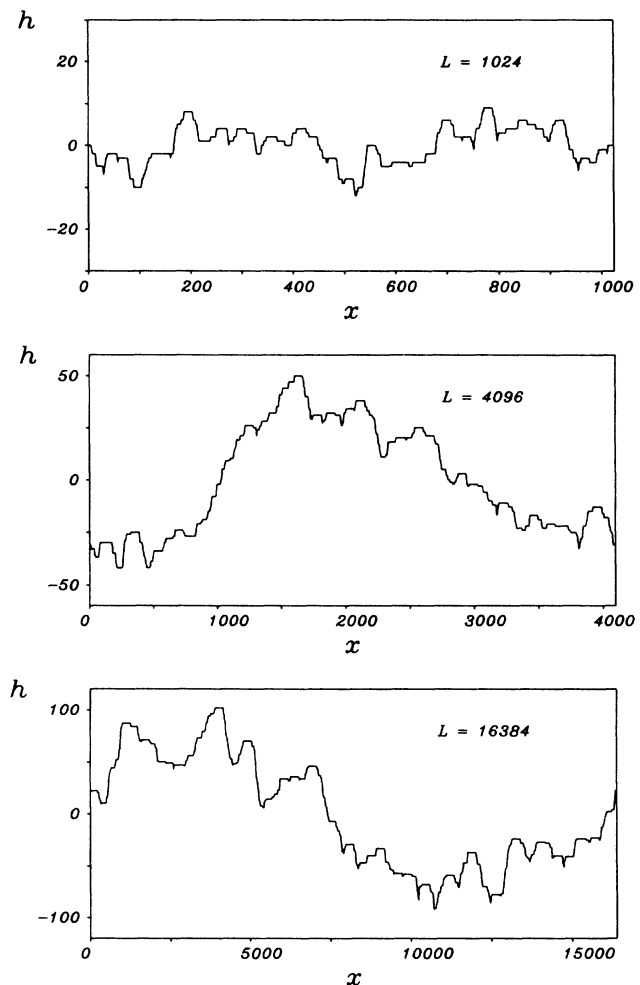
FIG. 2. Surface profiles generated from random initial data by the dynamics (3.1). The three plots show typical configurations at $t = 8$, 32, and 128. The correlation length is $\xi = L/64$ in all cases.

than ξ. But then, if the steps are more than ξ lattice spacings apart, they are uncorrelated, and thus their distance exceeds ξ by an amount proportional to the inverse density of steps. Since $\rho(t) \sim t^{-1/2}$, we conclude that the width of the local maxima is given by

$$l_{\max} = \xi + O(t^{1/2}) . \tag{3.24}$$

In comparison, the local surface minima are much narrower. Indeed, there is no lower bound on the distance between an upward step and a downward step to the *left* of it. The distribution function for the width of the local minima is approximately calculated in Appendix B. Normalized to unity, the result is

$$P_t(l) = \begin{cases} \dfrac{1}{\sqrt{l\xi}} \dfrac{\left[1 - \dfrac{l}{\xi}\right]}{\left[1 + \dfrac{l}{\xi}\right]^2} & \text{if } l \leq \xi \\ 0 & \text{if } l \geq \xi . \end{cases} \tag{3.25}$$

The distribution is thus concentrated at small l, with the first moment

$$\langle l_{\min} \rangle = (\pi - 3)\xi \simeq 0.14\xi . \tag{3.26}$$

The drastic difference between local maxima and minima gives a first quantitative measure of the asymmetry of the surface. For a more complete description of the effect, we consider moments of the quantity

$$\mu(l,t) := \tfrac{1}{2}[2h_0(t) - h_l(t) - h_{-l}(t)] . \tag{3.27}$$

μ describes the height fluctuations at the origin relative to a local mean height defined by

$$\bar{h}(l,t) = \tfrac{1}{2}[h_l(t) + h_{-l}(t)] . \tag{3.28}$$

Since we are interested in the surface asymmetry, we must compute odd moments of (3.27). More specifically, we want to calculate the local surface skewness[21] defined by

$$s(l,t) := \frac{\langle \mu(l,t)^3 \rangle}{\langle \mu(l,t)^2 \rangle^{3/2}} . \tag{3.29}$$

It is easy to check that s is negative for a surface composed of convex arcs. Furthermore, one expects $|s(l,t)|$ to have a maximum when l equals the typical arc length.

While the denominator in (3.29) is closely related to $\chi(l,t)$, the calculation of $\langle \mu^3 \rangle$ clearly involves the three-point step correlation function

$$D(x,y,t) := \langle \sigma_{-x}(t)\sigma_0(t)\sigma_y(t) \rangle . \tag{3.30}$$

The calculation of (3.30) is sketched in Appendix A. The result is

$$D(x,y,t) = \frac{1}{(2\pi^3)^{1/2}} \frac{1}{\sqrt{xy\xi}} \tilde{f}(x/\xi, y/\xi) \tag{3.31}$$

for $x,y \geq 0$ with

$$\tilde{f}(\lambda, \lambda') = \begin{cases} \dfrac{\lambda' - \lambda}{(1+\lambda)(1+\lambda')} & \text{if } 0 < \lambda, \lambda' < 1 \\ 0 & \text{otherwise} . \end{cases} \tag{3.32}$$

To proceed, we first note that

$$\langle \mu(l,t)^3 \rangle = \tfrac{3}{4}\langle [h_0(t) - h_l(t)][h_0(t) - h_{-l}(t)]^2 \rangle \tag{3.33}$$

since the third-order terms $[h_0(t) - h_{\pm l}(t)]^3$ vanish due to symmetry. Some further manipulations show that

$$\langle \mu(l,t)^3 \rangle = -\tfrac{3}{2} \int_0^l db \int_b^{l+b} dx \int_0^{l-b} dy \, D(x,y,t) . \tag{3.34}$$

The evaluation of the integral is tedious but fairly straightforward. We only present the final result for $s(l,t)$. Since s is a dimensionless quantity, cf. (3.29), statistical self-similarity (3.22) requires that it is a function only of l/t. Indeed, the result can be written as

$$s(l,t) = -\tilde{s}(l/\xi(t)) , \tag{3.35}$$

with $\tilde{s} > 0$. As $s(l,t)$ has no explicit time dependence, it is a true invariant of the surface dynamics. The scaling function $\tilde{s}$ is given by

$$\tilde{s}(\lambda) = \begin{cases} -3\sqrt{2}\left[\dfrac{A(\lambda)}{B(\lambda)^{3/2}}\right] & \text{for } 0 \leq \lambda \leq \tfrac{1}{2} \\[4mm] -3\sqrt{2}\left[\dfrac{A(\lambda) + 2\lambda \arctan\sqrt{2\lambda-1} - \sqrt{2\lambda-1} - \dfrac{\pi}{6}(2\lambda-1)^{3/2}}{B(\lambda)^{3/2}}\right] & \text{for } \tfrac{1}{2} \leq \lambda \leq 1 \\[4mm] -3\sqrt{2}\dfrac{(\pi/3 - 1)}{\left\{\dfrac{\pi}{2}\left[\lambda - \left[\dfrac{6}{\pi} - \dfrac{3}{2}\right]\right]\right\}^{3/2}} & \text{for } \lambda > 1 , \end{cases} \tag{3.36}$$

where

$$A(\lambda) = \int_0^{\min(\lambda, 1-\lambda)} d\mu (\sqrt{\lambda+\mu} \arctan\sqrt{\lambda-\mu} - \sqrt{\lambda-\mu} \arctan\sqrt{\lambda+\mu}) \tag{3.37}$$

and

$$B(\lambda) = \begin{cases} 4(1+\lambda)\arctan\sqrt{\lambda}-(2\lambda+1)\arctan\sqrt{2\lambda}-(4-\sqrt{2})\sqrt{\lambda} & \text{for } 0 \le \lambda \le \frac{1}{2} \\ 4(1+\lambda)\arctan\sqrt{\lambda}-4\sqrt{\lambda}-\dfrac{\pi}{2}\lambda+1-\dfrac{\pi}{4} & \text{for } \frac{1}{2} \le \lambda \le 1 \ . \end{cases}$$ (3.38)

$\bar{s}(\lambda)$ is a smooth function with a single maximum at $\lambda=0.55$, where it takes the value $\bar{s}_{\max}=0.47$ (Fig. 3). For small λ, $\bar{s}(\lambda)$ grows as $\lambda^{3/4}$, while the decay for $\lambda \to \infty$ is algebraic, cf. the last line in (3.36).

It is tempting to speculate whether a nonzero local surface skewness could be a general characteristic of surface growth models with a symmetry-breaking term like the nonlinearity in (2.3). Wolf[21] investigated the *global* skewness, i.e., (3.29) with $l=L$, for the Eden model. He observed changes of sign as a function of time but was unable to extract the asymptotic behavior. On the other hand, for the two-dimensional single-step model, the steady state is explicitly known to possess reflection symmetry.[2,3] We have performed some preliminary simulations of two-dimensional standard ballistic deposition and found a negative surface skewness of the same order of magnitude as in the present model, on a length scale of 10–20 lattice spacings.[16] We are further investigating this point, as well as the possible relevance of our findings for the experimentally observed microstructure in thin-film deposits.[22]

Let us add that both $\mathcal{X}(l,t)$ and $s(l,t)$ have been computed by a direct numerical simulation of Eq. (3.1). Provided that the correlation length ξ is much smaller than the system size L, we find excellent quantitative agreement with the analytical expressions (3.19) and (3.36). The additional effects which occur when $\xi \simeq L$ will be the topic of the next section.

D. Finite-size scaling

In equilibrium critical phenomena, finite-size effects set in when the correlation length becomes of the order of the system size. In the present model, the correlation length grows linearly with time according to (3.15). Thus we expect, for a system of size L, a time scale $T \sim L$, such that the asymptotic laws derived for the infinite system
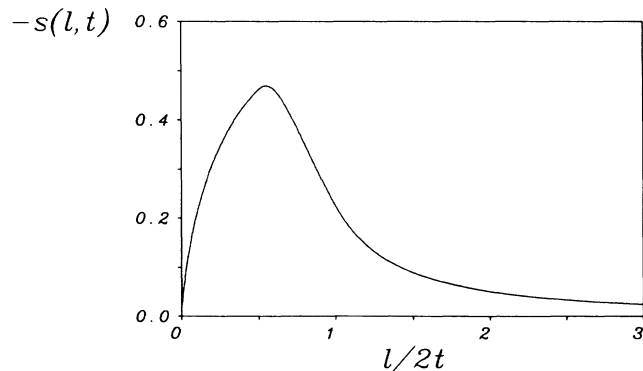
FIG. 3. Skewness scaling function as given by Eqs. (3.36)–(3.38).

cease to be valid when t approaches T. In fact, this statement can be made precise without any further calculation. To see this, we pick a typical initial configuration. Its maximum consists of a pair of an upward and a downward step at adjacent lattice sites. Under the dynamics the steps move apart and, due to the periodic boundary conditions, they will annihilate each other after $L/2$ time steps. Since this is the last pair of steps that vanishes, we conclude that the surface becomes totally flat at time $t=L/2$. Thus the relaxation time T is given by

$$T = L/2$$ (3.39)

in accordance with the scaling theory of Sec. II and $z=1$.

Let us now investigate in more detail how the step density $\rho(t)$ crosses over from the power-law decay (3.12) for $t \ll T$ to the flat surface, $\rho=0$, for $t=T$. In addition to (3.11), the random walks contributing to ρ at time t must then satisfy the periodic boundary conditions (3.3). The calculation of $\rho(t)$ for the restricted ensemble is given in Appendix C. The result is a simple modification of (3.12), namely,

$$\rho(t,L) = \frac{1}{\sqrt{\pi t}}\sqrt{1-t/T} \ ,$$ (3.40)

where, of course, t/T may be replaced by ξ/L.

Next we consider the mass deposited per unit area up to time t, related to the step density by (3.7). Inserting (3.40) into (3.7), we obtain for $t \le T$,

$$m(t,L) = m_{\max}(L)\tilde{F}(t/T) \ ,$$ (3.41)

where

$$m_{\max} = \sqrt{(\pi/8)L}$$ (3.42)

and

$$\tilde{F}(\lambda) = \frac{2}{\pi}[\arcsin(\sqrt{\lambda})+\sqrt{\lambda}\cos(\arcsin\sqrt{\lambda})] \ .$$ (3.43)

The expression (3.42) for the total mass deposited up to $t=T$ has a simple interpretation. Consider again a typical initial configuration h_x of length L. With the periodic boundary conditions, we may shift the boundaries in such a way that h_x takes on its absolute maximum $h_{\max}$ at $x=0$ and $x=L$. Then h_x forms a pit which is simply filled up with particles during the growth process. The total deposited mass, $m_{\max}L$, thus equals the volume of the pit, i.e., the area under the graph of $h_{\max}-h_x$:

$$m_{\max} = \frac{1}{L}\int_0^L dx \, \langle (h_{\max}-h_x) \rangle = \langle h_{\max} \rangle$$ (3.44)

and a simple calculation shows that $\langle h_{\max} \rangle$ agrees with (3.42). The scaling of $m_{\max}$ with L was anticipated in (2.12). For $t \ll T$, (3.41) reduces to

$$m(t) = \frac{2}{\sqrt{\pi}}\sqrt{t} \tag{3.45}$$

which confirms the general scaling form (2.10). Finally we note that the scaling function (3.43) approaches its saturation value $\bar{F}(1) = 1$ as

$$\bar{F}(1-\epsilon) \simeq 1 - \frac{4}{3\pi}\epsilon^{3/2} . \tag{3.46}$$

Both (3.40) and (3.41) were confirmed by direct numerical simulation. In fact, we expect a finite-size scaling form similar to (3.40) and (3.41) to hold for the time evolution of any well-defined quantity in our model. As an example, we calculated numerically the mean-square surface fluctuation

$$w(t,L)^2 = \frac{1}{L}\sum_{i=1}^{L}[h_i(t) - \bar{h}(t)]^2 , \tag{3.47}$$

where $\bar{h}(t)$ is the mean surface height

$$\bar{h}(t) = \frac{1}{L}\sum_{i=1}^{L}h_i(t) . \tag{3.48}$$

For $t = 0$, w^2 is given by (3.4), whereas clearly $w^2 = 0$ for $t \geq T$. Thus we expect the following scaling form:

$$w(t,L)^2 = \frac{L}{12}g(t/T) , \tag{3.49}$$

where $g(0) = 1$ and $g(1) = 0$. We note that (3.49) is exactly of the form (1.1) with $\zeta = \frac{1}{2}$ and $z = 1$, although the scaling function is different in the stochastic case. While we did not push to calculate the scaling function g analytically, the numerical data for various values of L displayed in Fig. 4 clearly demonstrate that such a scaling function exists.
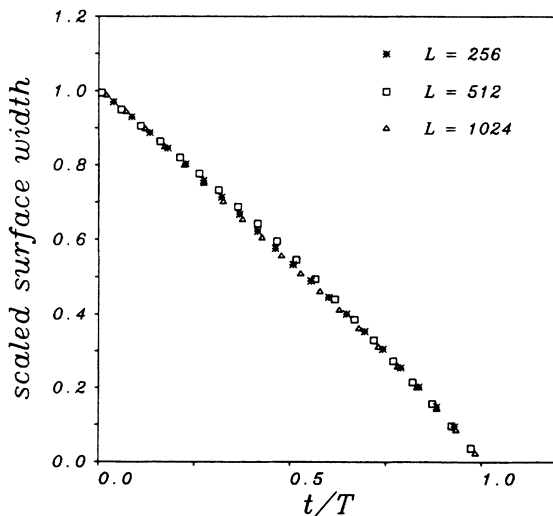
FIG. 4. Numerical data for the surface width $w(t,L)$ scaled according to (3.49). Each set of data points was obtained by averaging over 400 initial configurations.

IV. DETERMINISTIC EDEN GROWTH

Among the local growth rules, the one introduced by Eden[23] has been most thoroughly studied.[4,5] In the simplest version of the model, a new particle is added to a randomly chosen empty perimeter site of the cluster. In order to reduce the corrections to scaling of the surface width, Wolf and Kertész[24] developed the method of noise reduction. A counter is put at every growth site (=empty perimeter site). Each time the site is chosen by the random-number generator, the counter is incremented by one. When the counter reaches a prescribed value m, the growth site is filled and the counter is reset to zero. As $m \to \infty$, the growth proceeds layer by layer. The growth rule may then be formulated deterministically, and simply amounts to filling all available growth sites simultaneously. The model becomes a cellular automaton of the kind studied by Packard and Wolfram in two dimensions.[25]

In this section we outline the connection between the deterministic ($m = \infty$) two-dimensional Eden model and the lattice model (3.1). It will turn out that depending on the growth rule and the orientation of the substrate, deterministic Eden growth is either a trivial displacement of the surface as a whole, or it is described by (2.3) with $\beta = 1$. We will also gain some insight into the physical significance of the nonlinearity in (2.3).

Let us first rewrite (2.3), for a one-dimensional surface, in terms of the surface gradient $u = \partial h/\partial x$. Then

$$\frac{\partial}{\partial t}u(x,t) = D\frac{\partial^2}{\partial x^2}u(x,t) + \lambda c(u(x,t))\frac{\partial}{\partial x}u(x,t) , \tag{4.1}$$

where

$$c(u) = \beta\,\mathrm{sgn}(u)\,|u|^{\beta-1} . \tag{4.2}$$

Equation (4.1) is a diffusion equation with a nonlinear convection term. A piece of the surface with slope u is translated along the x axis with velocity $c(u)$. For layerwise growth, $c(u)$ is related to the directional dependence of the normal growth velocity. We consider a sharp corner where two straight surface segments meet. One segment is parallel to the x axis and the other one is tilted by an angle ϕ, cf. Fig. 5. Let v_0 be the growth velocity normal to the x axis, and $v(\phi)$ the normal velocity of the tilted segment. After one unit of time, the position of the corner is then shifted by an amount $\Delta(\phi)$ along the x axis. The geometric construction in Fig. 5 gives

$$\Delta(\phi) = \frac{v(\phi) - v_0\cos\phi}{\sin\phi} . \tag{4.3}$$

Clearly, $\Delta(\phi)$ can be identified with the convection speed $c(u)$. If the growth velocity is independent of the slope, $v(\phi) \equiv v_0$, then $\Delta(\phi) \simeq \frac{1}{2}v_0\phi$ for small ϕ. Thus $c(u) \sim u$ and $\beta = 2$. This is the derivation of (1.2) for lateral growth as given in Ref. 9.

However, for deterministic Eden growth, $v(\phi)$ depends on the orientation. If the x axis is chosen as the lattice axis of a square lattice, the normal growth velocity for the standard nearest-neighbor (NN) Eden model is

$$v(\phi) = \max(\,|\sin\phi|\,,\,|\cos\phi|\,) \tag{4.4}$$
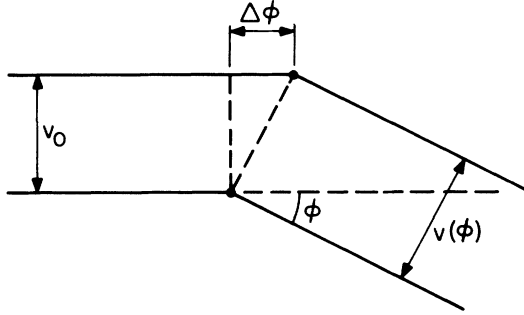
FIG. 5. Geometric construction used to calculate the horizontal displacement of a surface step in layer-wise growth.

FIG. 6. Orientational dependence of the normal growth velocity for the deterministic NN and NNN Eden models.

on the circle $-\pi \leq \phi \leq \pi$. To discuss growth from a substrate parallel to the x axis, we may restrict ourselves to the range $|\phi| \leq \pi/4$. Since overhangs and high steps are strongly suppressed by noise reduction,[24] the initial surface configurations contain no segments with more than unit slope $|\tan\phi| \leq 1$. Within this range, $v(\phi) = \cos\phi$ and therefore $\Delta(\phi) \equiv 0$. Thus the corners do not propagate, and the dynamics is a trivial displacement of the surface $h_i(t+1) = h_i(t) + 1$.

For comparison, we introduce the next-nearest-neighbor (NNN) Eden model, where both the nearest and the next-nearest neighbors of an occupied site are possible growth sites. In the deterministic limit, the normal growth velocity is now

$$v(\phi) = |\cos\phi| + |\sin\phi| \ . \tag{4.5}$$

Inserting this into (4.3) gives, for $|\phi| \leq \pi/4$,

$$\Delta(\phi) = \text{sgn}(\phi) \ . \tag{4.6}$$

Thus $c(u) \sim \text{sgn}(u)$, and the surface relaxes with a nonlinearity exponent $\beta = 1$. In fact, the growth rule for the deterministic NNN Eden model may be written as

$$h_i(t+1) = \max(h_{i-1}(t), h_i(t), h_{i+1}(t)) + 1 \tag{4.7}$$

which is identical to (3.1).

Why are the NN and the NNN rules so different? In Fig. 6 we show polar plots of $v(\phi)$ for the two models. Apparently, the plots are equivalent up to a rotation of $\pi/4$. Indeed, if one considers growth from a substrate parallel to the lattice diagonal, the properties of the two models are interchanged. Now the NNN rule is trivial, whereas the NN rule leads to surface relaxation. Thus the directions of nontrivial (relaxational) growth dynamics are associated with the cusps in $v(\phi)$. Wolf[21] has shown that the asymptotic shape of an Eden cluster is determined by $v(\phi)$ through the well-known Wulff construction. Accordingly the cusps in $v(\phi)$ give rise to facets in the asymptotic cluster shape, which is a diamond for the NN rule, and a square for the NNN rule.[25] In that sense, we see that (2.3) with $\beta = 1$ describes the growth of facets on an initially rough crystal surface.
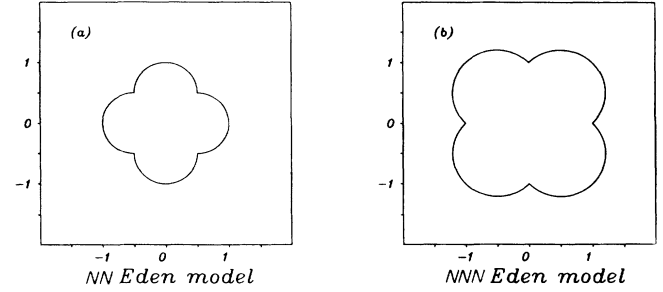
V. CONCLUSIONS

We have studied deterministic surface growth and achieved (i) a general scaling theory and (ii) an unusually detailed analysis of the deterministic KPZ equation with nonlinearity $|(\partial/\partial x)h(x,t)|$. We want to comment on two issues. (i) How are Burgers's results related to ours? (ii) What do we learn about the stochastic growth?

(i) If in the deterministic KPZ equation we set $u(x,t) = (\partial/\partial x)h(x,t)$, then u is governed by the Burgers equation

$$\frac{\partial}{\partial t}u(x,t) = D\frac{\partial^2}{\partial x^2}u(x,t) + \lambda\frac{\partial}{\partial x}u(x,t)^2 \ . \tag{5.1}$$

Since, at time $t = 0$, $h(x)$ is the graph of a random walk, its increments $u(x)$ are stationary and essentially uncorrelated. One has to solve then (5.1) subject to these random initial data. This is precisely the problem investigated by Burgers.[10] He shows that in the long-time limit $u(x,t)$ is composed of linear pieces with slope $-1/t$ separated by shock discontinuities. The shocks move at constant velocity. Upon collision they coalesce and continue with a new velocity. The surface height $h(x,t)$ consists therefore of downwards parabolas joined at kink discontinuities. Their curvature flattens out in the course of time. Burgers showed that $\langle |u(x,t)| \rangle \cong t^{-1/3}$ and that the typical arc length increases as $t^{2/3}$. This fits with our general scaling theory: Since $\zeta = \frac{1}{2}$, $\beta = 2$, we must have

$$z = \frac{3}{2} \tag{5.2}$$

and a $t^{-1/3}$ decay of the step density. According to Burgers, "$\langle u(x,t)u(y,t)\rangle$ becomes so complicated, that there is little hope for its evaluation." So why could we do better for our case? With nonlinearity $|(\partial/\partial x)h(x,t)|$ the surface gradient is governed by

$$\frac{\partial}{\partial t}u(x,t) = D\frac{\partial^2}{\partial x^2}u(x,t) + \lambda\frac{\partial}{\partial x}|u(x,t)| \ . \tag{5.3}$$

Now the characteristics have only velocity $\pm\lambda$, in contrast to Burgers's equation, where they have a general velocity $2\lambda u(x)$. Clearly, this latter case is more difficult.

(ii) When starting our investigation we hoped that the deterministic growth would yield some information about the dynamical exponent z of the stochastic KPZ equa-

tion. Now we see that this hope is futile, although in a somewhat subtle way. Within our general scaling theory we recover, for $\beta=2$, the scaling law (2.14) relating the static and dynamic exponent in the stochastic case.[11,13] However, the significance of the static exponent ζ is quite different in the two cases: For stochastic growth ζ is the static scaling exponent of the steady state and thus given indirectly by the dynamics. For deterministic growth ζ is given by the initial conditions. Therefore the deterministic case can teach us only how the dynamic and static exponent are coupled, but not their specific numerical value.

Moreover, as we mentioned at the end of Sec. III B, the nonlinearity exponent β could be affected by the noise. While the stochastic growth models studied so far appear to belong to the $\beta=2$ universality class,[1-5] ignoring the trivial cases of diffusive relaxation[6,7] and random deposition,[1,6] one cannot exclude the possibility of a stochastic growth rule leading to a value of β other than 2. Following the arguments of Sec. IV such a rule would be expected to display strong lattice anisotropy even under the influence of noise. The derivation of the correct form of the nonlinearity from a given growth rule is a nontrivial problem which clearly requires further investigation.

Note added in proof. The following two articles have been brought to our attention: one by Kida[25] studies the deterministic Burgers equation $(\beta=2)$ with random initial data corresponding to the two cases $\zeta=0$ and $1/2$; the other by Elskens and Frisch[26] also derives the decay of the average step density, Eq. (3.12).

ACKNOWLEDGMENTS

APPENDIX A: DERIVATION OF STEP CORRELATION FUNCTIONS

We want to compute the probability for finding, at time t, two particles at a relative distance l. By translational invariance we may assume the positions of the particles to be $x=t$ and $x=t+l$. The history of the particles then depends on the initial data in the intervals $[0,2t]$ and $[l,l+2t]$, respectively, as shown in Fig. 7. In particular, if these intervals do not intersect, i.e., if $l>2t$, the particles are statistically independent and (3.17) holds. Clearly this is a consequence of the short-range correlations among the $\sigma_i(0)$.

The correlation function (3.13) decomposes into four terms, corresponding to the possible combinations of velocities of the two particles. Let us first consider the case when both particles have velocity $+1$. Then at $t=0$ their positions were $x=0$ and $x=l$. Let $h(x)$ denote the initial condition and fix it at the origin, $h(0)=0$. Then both particles survive up to time t if

$$h(x)<0 \quad \text{for } x\in[0,2t] \tag{A1a}$$

and

$$h(x')<h(l) \quad \text{for } x'\in[l,l+2t] . \tag{A1b}$$

Our goal is to compute the relative weight of initial profiles which satisfy (A1) within the ensemble of all one-dimensional random walks. Let us denote by $Q_T(x,x')$ the probability for a random walk to go from x to x', $x'<x$, in time T without returning to x. Setting $y:=h(l)$ and $z:=h(l+2t)$ the weight of a random walk which satisfies (A1) is then

$$W(y,z)=Q_l(0,y)Q_{2t}(y,z) , \tag{A2}$$

where $0>y>z$. To obtain the total contribution to the correlation function, we must integrate (A2) over the admissible range of y and z, i.e.,

$$G^{++}(l,t)=\int_{-\infty}^{0} dy \int_{-\infty}^{y} dz\, Q_l(0,y)Q_{2t}(y,z) . \tag{A3}$$

The contribution from two particles with velocity -1 is identical to (A3) as can be seen from a symmetry transformation.

Next we consider the case when the left particle has velocity $+1$ and the right particle has velocity -1. Then the initial positions are $x=0$ and $x=l+2t$ and the particles approach each other. Fixing again $h(0)=0$, the condition for the initial profile is

$$h(x)<0 \quad \text{for all } x\in[0,2t] \tag{A4a}$$

and

$$h(x')<h(l+2t) \quad \text{for all } x'\in[l,l+2t] . \tag{A4b}$$

Here we must discriminate between $z=h(l+2t)>0$ and $z<0$. If $z>0$, then (A4a) implies (A4b) within the overlap interval $[l,2t]$, and the weight of an admissible walk is

$$W_1(y,z)=Q_{2t}(0,y)Q_l(y,z) , \tag{A5}$$

where $y=h(2t)<0$. If $z<0$, (A4b) implies (A4a) in $[l,2t]$, and the weight is

$$W_2(y',z)=Q_l(0,y')Q_{2t}(y',z) \tag{A6}$$

and now $y'=h(l)<z$. Taken together, we obtain the following contribution to the correlation function:
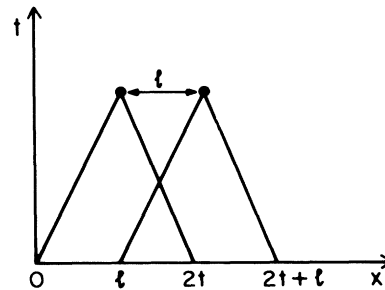
FIG. 7. Space-time diagram used in the derivation of the step correlation functions in Appendix A.

$$G^{+-}(l,t) = -\left[\int_0^\infty dz \int_{-\infty}^0 dy \, Q_{2t}(0,y)Q_l(y,z) \right.$$
$$\left. + \int_{-\infty}^0 dz \int_{-\infty}^z dy' \, Q_l(0,y')Q_{2t}(y',z) \right] .$$

$$\text{(A7)}$$

G^{+-} is negative since the particle velocities have different signs.

The last case to consider is the one where the two particles move apart at time t. Then initially the left particle was at $x = 2t$ and the right particle at $x = l$. But since $l < 2t$, this implies that their trajectories must have crossed, and thus they cannot be present at time t. We conclude that these pairs do not contribute to the correlation function. Stated differently, this implies that a local surface maximum at time t must have a width of at least $2t$, cf. Eq. (3.24).

In order to evaluate the integrals (A3) and (A7) we must still specify the propagator $Q_T(x,x')$. We will use a continuum approximation, which becomes exact when $x,x' \gg 1$ and $T \gg 1$. Then, for $x' < x$,

$$Q_T(x,x') = \frac{1}{(2\pi T^3)^{1/2}}(x-x')e^{-(x-x')^2/2T} . \quad \text{(A8)}$$

Inserting this into (A3) and (A7) and adding up the different contributions according to

$$G(l,t) = 2G^{++}(l,t) + G^{+-}(l,t) \quad \text{(A9)}$$

one obtains (3.14).

The computation of the three-point function (3.30) proceeds along the same lines. Again the correlations vanish if the distance between any two particles exceeds $2t$. There are eight contributions to the correlation function, corresponding to the different combinations of particle velocities. However, now the $(+++)-$ and the $(---)-$ terms have different signs and thus cancel. Furthermore, since no left-going particle can be within $2t$ to the left of a right-going particle, the terms $(-+-)$, $(--+)$, $(-++)$, and $(+-+)$ also vanish. One is left with two terms which are related by a change of sign and an exchange of the arguments (x,y), i.e.,

$$D(x,y) = f(x,y) - f(y,x) , \quad \text{(A10)}$$

with

$$f(x,y) = \left[\int_{-\infty}^0 da \, Q_x(0,a) \int_a^\infty dc \int_{-\infty}^a db \, Q_{2t}(a,b)Q_y(b,c) + \int_{-\infty}^0 da \, Q_x(0,a) \int_{-\infty}^a dc \int_{-\infty}^c db \, Q_y(a,b)Q_{2t}(b,c) \right] .$$

$$\text{(A11)}$$

APPENDIX B: DISTRIBUTION OF LOCAL SURFACE MINIMA

Here we want to identify those initial surface configurations which admit, at time t, a local minimum with a plateau of length l. The two steps which constitute the plateau were initially at a distance $l + 2t$ and at the same height h_0 which we set to $h_0 = 1$ in units of the lattice spacing. They approach each other and will annihilate at time $t + l/2$. Thus the initial surface configuration must satisfy

$$h(x) \le 0 \quad \text{for all } x \in [0, l + 2t] , \quad \text{(B1)}$$

where we have assumed that the left downward step starts at $x = 0$. Furthermore, since the plateau is to be completely flat at time t, all the surface fluctuations initially present between the two steps must have been smoothed by that time. This implies that the downward excursions of the initial configuration away from the $h = 0$ line cannot extend over more than $2t$ lattice spacings along the x axis. The most general random walk which contributes to a local minimum of width l at time t will thus return to the $h = 0$ line n times, $h(y_i) = 0$ for $i = 1, \ldots, n$, and the points of return will be distributed in the interval $[0, l + 2t]$ such that their differences $x_i = y_{i+1} - y_i$ for $i = 1, \ldots, n$ and $x_{n+1} := l + 2t - y_n$ satisfy

$$x_i < 2t, \quad i = 1, \ldots, n+1$$
$$\sum_{i=1}^{n+1} x_i = l + 2t . \quad \text{(B2)}$$

The propagator which takes the walk from y_i to y_{i+1} is

given by (A8) with $T = x_i$ and $x - x' = 1$. The contribution of all walks with n returns which satisfy (B2) is then

$$I_n(l,t) = \int_0^{2t} dx_1 \cdots \int_0^{2t} dx_{n+1} \left[\prod_{i=1}^{n+1} \frac{e^{-1/2x_i}}{(2\pi x_i^3)^{1/2}} \right]$$
$$\times \delta\left[\sum_{i=1}^{n+1} x_i - l - 2t \right] . \quad \text{(B3)}$$

Let us try to estimate the integral for large t. If each of the x_i is of the order t, the integrand is of the order $t^{-3(n+1)/2}$. The volume of integration, defined by (B2), is proportional to t^n. Together this implies

$$I_n(l,t) = O(t^{-(n+3)/2}) . \quad \text{(B4)}$$

Thus for large t the lowest order term, $n = 1$, dominates, and it is sufficient to compute $I_1(l,t)$.

When $n = 1$, then (B2) can be met only if $l \le 2t$. This implies that, to leading order in $t^{-1/2}$, all local minima have a width *smaller* than $2t$. With some rescaling of variables, the integral (B3) with $n = 1$ becomes

$$I_1(l,t) = \frac{1}{2\pi} T^{-2} \int_{l/T}^{2t/T} dz \frac{e^{1/[Tz(1-z)]}}{[z(1-z)]^{3/2}} , \quad \text{(B5)}$$

where $T := l + 2t$. Within the range of integration, the argument of the exponential function is always much less than unity. The exponential factor can thus be dropped, and one obtains

$$I_1(l,t) = \frac{2}{\pi}(2t)^{-3/2} l^{-1/2} \frac{1 - l/2t}{(1 + l/2t)^2} . \quad \text{(B6)}$$

Normalizing this to unity on the interval $[0, 2t]$ finally produces (3.25).

APPENDIX C: STEP DENSITY IN THE FINITE SYSTEM

As in Sec. III C, we consider a particle with velocity $+1$ which starts at the origin at time t. It survives up to time t if the initial configuration $h(x)$ satisfies

$$h(x) < 0 \quad \text{for all } x \in [0, 2t] . \tag{C1}$$

Here we have set $h(0) = 0$. In a finite system of length L with periodic boundary conditions, $h(x)$ has to satisfy

$$h(L) = h(0) = 0 \tag{C2}$$

in addition to (C1). On the interval $[2t, L]$, there is no restriction like (C1) on the random walk. The weight of such a walk may therefore be written as

$$W(y,t) = Q_{2t}(0,y) P_{L-2t}(y,0) , \tag{C3}$$

where $y = h(2t) < 0$, Q is defined in (A8), and

$$P_T(x,y) = \frac{1}{\sqrt{2\pi T}} e^{-(x-y)^2/2T} \tag{C4}$$

is the probability for an unrestricted random walk to go from x to y in time T. Taking the integral of (C3) over the intermediate positions $y < 0$ results in

$$\int_{-\infty}^{0} dy \, W(y,t) = \frac{1}{2\pi L} \left[\frac{L-2t}{2t} \right]^{1/2} . \tag{C5}$$

The *total* weight of walks which satisfy (C2) is clearly given by

$$P_L(0,0) = \frac{1}{\sqrt{2\pi L}} . \tag{C6}$$

Since we are interested in the probability of finding a particle at time t within the restricted set of initial conditions subject to (C2), we must normalize (C5) by (C6) to obtain

$$\rho^+(t,L) = \frac{1}{2} \frac{1}{\sqrt{\pi t}} \sqrt{1 - 2t/L} . \tag{C7}$$

Together with an identical contribution from particles with velocity -1 this adds up to (3.40).

---

*Permanent address: Theoretische Physik, Universität München, Theresienstrasse 37, D-8 München 2, West Germany.

[1]F. Family and T. Vicsek, J. Phys. A **18**, L75 (1985).

[2]P. Meakin, P. Ramanlal, L. M. Sander, and R. C. Ball, Phys. Rev. A **34**, 5091 (1986).

[3]M. Plischke, Z. Rácz, and D. Liu, Phys. Rev. B **35**, 3485 (1987).

[4]P. Meakin, R. Jullien, and R. Botet, Europhys. Lett. **1**, 609 (1986).

[5]D. E. Wolf and J. Kertész, Europhys. Lett. **4**, 651 (1987).

[6]F. Family, J. Phys. A **19**, L441 (1986).

[7]P. Meakin and R. Jullien, J. Phys. (Paris) **48**, 1651 (1987).

[8]S. F. Edwards and D. R. Wilkinson, Proc. R. Soc. London, Ser. A **381**, 17 (1982).

[9]M. Kardar, G. Parisi, and Y. C. Zhang, Phys. Rev. Lett. **56**, 889 (1986).

[10]J. M. Burgers, *The Nonlinear Diffusion Equation* (Riedel, Boston, 1974).

[11]J. Krug, Phys. Rev. A **36**, 5465 (1987).

[12]D. Dhar, Phase Transitions **9**, 51 (1987).

[13]M. Kardar and Y. C. Zhang, Phys. Rev. Lett. **58**, 2087 (1987).

[14]S. Wolfram, Rev. Mod. Phys. **55**, 601 (1983).

[15]R. Lipowsky and M. E. Fisher, Phys. Rev. Lett. **56**, 472 (1986); M. E. Fisher, J. Chem. Soc. Faraday Trans. 2 **82**, 1569 (1986).

[16]J. Krug (unpublished).

[17]H. van Beijeren, R. Kutner, and H. Spohn, Phys. Rev. Lett. **55**, 2026 (1985).

[18]P. Grassberger, Physica **10D**, 52 (1984).

[19]K. Kang and S. Redner, Phys. Rev. A **32**, 435 (1985).

[20]H. J. Herrmann, Phys. Rep. **136**, 154 (1986).

[21]D. E. Wolf, J. Phys. A **20**, 1251 (1987).

[22]H. J. Leamy, G. H. Gilmer, and A. G. Dirks, in *Current Topics in Materials Science,* edited by E. Kaldis (North-Holland, Amsterdam, 1980), Vol. 6.

[23]M. Eden, in *Proceedings of the Fourth Berkeley Symposium on Mathematical Statistics and Probability,* 1961, edited by F. Neyman (University of California, Berkeley, 1961), Vol. 4, p. 223.

[24]D. E. Wolf and J. Kertész, J. Phys. A **20**, L257 (1987); J. Kertész and D. E. Wolf, *ibid.* **21**, 747 (1988).

[25]S. Kida, J. Fluid Mech. **93**, 337 (1979).

[26]Y. Elskens and H. L. Frisch, Phys. Rev. A **31**, 3812 (1985).